



UDK 530.1

REGULARITIES OF WO₃ FILM FORMATION DURING THERMAL OXIDATION OF W(111) AND THEIR ELECTRONIC STRUCTURE

Yorkulov Ruslan Maxammadi o'g'li.

In physics and mathematics (PhD), associate professor

University of Economics and Pedagogy,

E-mail: ruyo1990@mail.ru

Биринчи марта юкори вакуум қурилмаларида термик оксидланиш йўли билан WO₃/W(111) нанопленкалари ҳосил бўлишининг оптимал шартлари аниқланди ва олинди. Бир хил стехиометрик таркибли WO₃ пленкалари T=1100 К да кислороднинг P=(1–5)×10⁻³ Па даги портциал босими остида W ни оксидлаб олинди. Оже – электрон спектроскопия, ультрабинафша фотоэлектрон спектроскопия ва ИЭЭ (иккиламчи электронлар эмиссияси) коэффицентларининг энергия бўйича боғлиқлик ёзуви усуллари билан фойдаланиб WO₃ нинг таркиби, валент электронлар зичлик ҳолати бўйича энергетик соҳалар параметрлари ўрганилди. WO₃ нинг валент электронлар зиклик ҳолатида W нинг 6s ва 5d электронлари кислороднинг 2p электронлари билан гибридлашиши туфайли E_{св}=0÷5 эВ интервалда 3 та максимумга эришади. Пленканинг тақиқланган соҳа кенглиги ~ 2,8 эВ ни ташкил қилади.

Калит сўзлар: оксидлаш, оже-электронлар, фотоэлектронлар спектри, эластик қайтган электронлар, оролчали ўсиш, зичлик ҳолати, тақиқланган соҳа кенглиги.

Впервые в сверхвысоковакуумном приборе получены и определены оптимальные условия формирования нанопленок WO₃/W(111) методом термического окисления. Наиболее совершенные пленки WO₃ получены при окислении W при T = 1100 К в атмосфере кислорода с парциальным давлением P = (1 – 5)×10⁻³ Па. С использованием методов оже-электронной спектроскопии, ультрафиолетовой фотоэлектронной спектроскопии и записи энергетических зависимостей коэффицентом вторичной электронной эмиссии изучены состав, плотности состояния валентных электронов и параметры энергетических зон WO₃. Установлено, что в плотности состояния валентных электронов WO₃ в интервале E_{св} = 0 – 5 эВ имеется три максимума сформированных вследствие гибридизации 6s и 5d электронов W с 2p электронами кислорода. Ширина запрещенной зоны пленки составляет ~ 2,8 эВ.

Ключевые слова: окисление, оже-электроны, фотоэлектронные спектры, упруго-отраженные электроны, островковый рост, плотность состояния, ширина запрещенной зоны.

For the first time in an ultra-high vacuum device, the optimal conditions for the formation of WO₃/W(111) nanofilms by thermal oxidation were obtained and determined. The most perfect WO₃ films were obtained by oxidizing W at T = 1100 K in an oxygen atmosphere with a partial pressure of P = (1–5)*10⁻³ Pa. The composition, densities of state of valence electrons and parameters of the energy bands of WO₃ were studied using the methods of Auger electron spectroscopy, ultraviolet photoelectron spectroscopy and recording of the energy dependences of the secondary electron emission coefficients. It was found that in the density of state of valence electrons of WO₃ in the range of E_b = 0 – 5 eV there are three maxima formed due to the hybridization of 6s and 5d electrons of W with 2p electrons of oxygen. The band gap of the film is ~ 2.8 eV.

Key words: oxidation, Auger electrons, photoelectron spectra, elastically reflected electrons, island growth, density of state, band gap.



Introduction

Semiconductor metal oxides such as WO_3 , MoO_3 with increased carrier mobility have great potential for nanoelectronics, photonics, catalysis, nanosensors and electrochromic applications [1 – 9]. In addition to graphene and metal dichalcogenides, 2D-substoichiometric WO_{3-x} is becoming increasingly important as a promising semiconductor material for devices based on field-effect transistors [1].

WO_3 is known to stimulate the interaction of various gases and vapors on its surface and changes its properties, which are manifested in electro- and photochromic effects [10]: a change in the optical refractive index that occurs during structural rearrangement of the oxide due to electron and ion transfer. Changes in the optical properties of tungsten trioxide-based systems under the influence of gas environments are of interest due to the need to create indicators for monitoring the content and utilization of the corresponding gases in real conditions [10].

In addition, WO_3 is a catalyst for the decomposition of ammonia into nitrogen and hydrogen [11], and on the (100) faces of the tungsten crystal lattice, catalytic dissociation of molecular hydrogen and nitrogen to an atomic state occurs [12].

Currently, various methods are used to synthesize WO_3 : hot-wire metal oxide deposition [13]; microwave deposition [14], reactive magnetron sputtering [15], and ion implantation [16, 17]. These studies also studied the mechanisms of tungsten oxide formation. Previously, we obtained Si and Mo oxide nanofilms using thermal oxidation and ion implantation and studied their composition and electronic structures.

This work is devoted to studying the patterns of WO_3 nanofilm formation during thermal oxidation of W in an O_2 environment and studying their energy

band parameters and the electron state density of the valence band.

Experimental Procedure

The composition and electronic properties of the surface of the materials were studied using Auger electron spectroscopy (AES), elastically reflected low energy electron spectroscopy ($-dR/dE_p$ dependence on the energy of primary electrons E_p), and ultraviolet photoelectron spectroscopy (UPES). An Auger spectrometer with a small-angle analyzer of the Hughes–Rozhansky type was used in the work. The sensitivity of the Auger spectrometer in detecting impurities is 0.05–0.1%. The total error in determining the position of the Auger peaks in the spectrum does not exceed 0.8–1 eV. The depth of analysis by the AES and UPES methods is $\sim 5\text{--}10 \text{ \AA}$. The energy position of the EPES and elastically reflected electron peaks was determined with an error of 2–3%. The distribution profiles of Ba atoms were obtained by the AES method in combination with surface etching with Ar^+ ions.

Results And Discussion

To obtain WO_3 nanofilms by thermal oxidation, the W(111) surface was first maximally cleaned by heating to $T = 2100 \text{ K}$ for 5–6 hours under a vacuum of no worse than 10^{-7} Pa . Then oxygen was admitted to the device compartment. Fig. 1, a shows the dependence of the oxygen Auger peak intensity I_0 on the W oxidation time at $T = 1100 \text{ K}$ at different oxygen partial pressures from 10^{-2} to $5 \times 10^{-4} \text{ Pa}$. It is evident from Fig. 1 that with increasing $P_{(\text{O}_2)}$ the formation time of the WO_3/W film decreases. However, an increase in $P_{(\text{O}_2)}$ to 10^{-2} Pa leads to some deterioration in the stoichiometric composition (the appearance of an oxide of the WO_4 type) of the surface, and at $P_{\text{O}_2} \leq 10^{-3} \text{ Pa}$ the WO_3 formation rate decreases significantly. In our case, the optimal P_0 was found to be within the range of $5 \times 10^{-3} - 10^{-3} \text{ Pa}$.

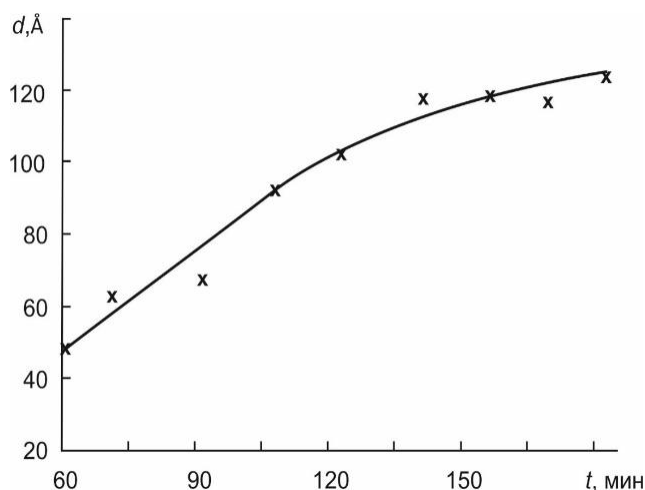


Fig. 1. Dependences of the surface concentration of O at different partial pressures of oxygen on the oxidation time of W at $T = 1100$ K (a) and the dependence of the thickness of the WO_3 film on the oxidation time of W(111) in an oxygen atmosphere with a pressure of 5×10^{-3} Pa at $T = 1100$ K (b)

The analysis of the OES results together with the SEM data showed that in the initial stage of oxidation ($t \leq 50 - 60$ min) island growth of the WO_3 film is observed. WO_3 films uniform over the surface at $P_{O_2} = 5 \times 10^{-3}$ Pa with a thickness of $\sim 40 - 50$ Å are formed at $t = 60 - 70$ min. Further increase in t leads to an increase in the thickness of the homogeneous film. From Fig. 1, b it is evident that the growth of d in the range $t = 60 - 120$ min occurs linearly, at a rate of ~ 1 Å/min. At $t \geq 120$ min the growth rate slows down and at $t = 150$ min $d_{WO_3} = 120$ Å. At $t \geq 150$ min with increasing t the value of d slowly monotonically increases. Figure 2 shows the spectra (energy distribution curves (EDC)) of

photoelectrons of pure W and a WO_3/W film with a thickness of 200 Å, measured at a photon energy of $h\nu = 15.6$ eV. It is known that the structure of the EDC of photoelectrons reflects the distributions of the density of states of the valence band electrons. In the case of W, the spectrum contains maxima at $E_b = -0.5; -1.8$ and -4.2 eV, apparently due to the excitation of electrons from the surface states (SS) and from the $6s$ and $5d$ states of the valence band electrons, respectively. There is also a weak feature at $E_b = -8.0$ eV, characteristic of unbound oxygen atoms. The spectrum of WO_3 contains maxima at $E_b = -3.6; -5.9$ and -7.7 eV, apparently due to the hybridization of the $6s$ energy levels of tungsten and $2p$ of oxygen.

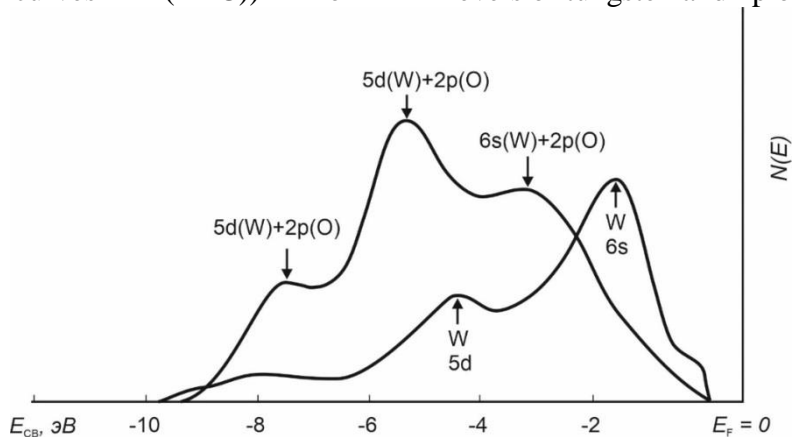


Fig. 2. UV-PES of a single-crystal sample of W (111) (curve 1) and a WO_3/W (111) film with $\Theta = 200$ Å (curve 2)



In this case, all the maxima of W , including the maxima associated with surface states, completely disappear. The main parameters of the energy bands can be determined from these spectra. The position of the valence band ceiling E_V was determined using the formula $h\nu = \Delta E + \Phi$ [91, 92 All]. The position of the Fermi level E_F is determined relative to E_F of pure W . To determine the width of the band gap, the method of recording the $R(E_p)$ and $\delta(E_p)$ dependences in the low-energy region was used (Fig. 3). Where R is the coefficient of elastically reflected electrons (ERE), E_p is the coefficient of truly secondary electrons (TSE), and E_p is the energy of primary electrons. The course of these dependences is directly related to the band-energy structure of the

sample under study [18 – 20]. In all cases, a sharp decrease in R is due to the occurrence of an inelastic process, i.e. the transition of electrons from the valence band to the conduction band or to a vacuum.

It is evident that the onset of the inelastic process occurs at $E_{p\eta} = 2.8$ eV, apparently due to the transition of electrons from the top of the valence band E_v to the bottom of the conduction band E_c . These values are equal to the band gap width E_g . The second sharp decrease in R is observed at $E_{p\delta} = 6.2$ eV, and it corresponds to the initial sharp increase in the coefficient of true secondary electrons δ . From this it is evident that the decrease in R is associated with the transition of electrons from E_v to the vacuum level E_B .

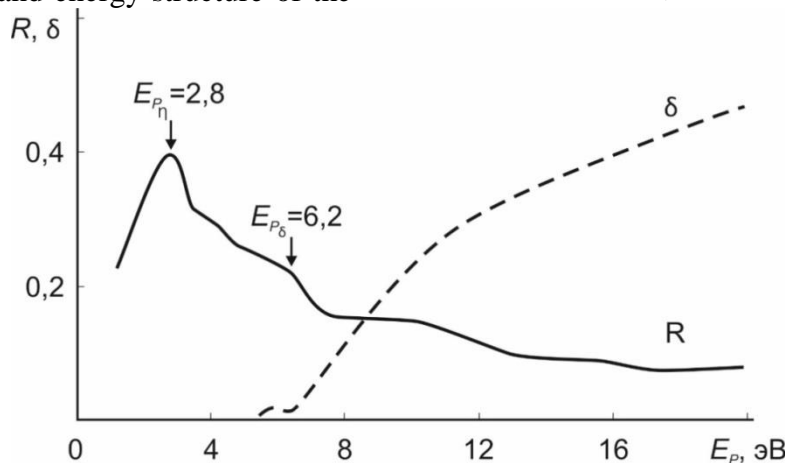


Fig. 3. Dependences of the coefficients R and δ on E_p for WO_3 film

Based on the analysis of Fig. 2 and 3, the main parameters of the energy bands of the WO_3 film were determined (Table 1). For

comparison, the band parameters of the WO_2 and $W(111)$ films are also given here.

Table 1.

Band-energy parameters of $W(111)$, $WO_3/W(111)$ and $WO_2/W(111)$ with $d=250 \text{ \AA}$

Parameters	$E_V, \text{ eV}$	$E_F, \text{ eV}$	$E_g, \text{ eV}$	$\chi, \text{ eV}$
Sample				
$W(111)$	4,3	4,3	0	4,3
WO_3	6,2	4,3	2,8	3,4

From the table it is clear that WO_3 and WO_2 films are wide-bandgap semiconductors.



Conclusion

O₃ films of different thickness were obtained by thermal oxidation of W(111) in an ultrahigh vacuum device. It was shown that island growth of the WO₃ film is observed at the initial stage of oxidation. The experimental results showed that the most homogeneous WO₃ films are formed at a substrate temperature of 1100 K in an oxygen atmosphere with a pressure of P_{O₂} ≈ (1-5) × 10⁻³ Pa. It was found that WO₃ films have the properties of a wide-band semiconductor.

For the first time, information was obtained on the density of state of the valence band electrons and the parameters of the energy bands of WO₃/W (111) nanofilms obtained by thermal oxidation were determined.

Literature

1. Serge Zhuiykov et al. / *Nanoscale*, 2014, 6, 15029 DOI:10.1039/C4NR05008H – Proton intercalated two-dimensional WO₃ nano-flakes with enhanced charge-carrier mobility at room temperature – Интеркалированные протонами двумерные наночастицы WO₃ с повышенной подвижностью носителей заряда при комнатной температуре
2. Yang Y.A, Y.W.Cao, B.N. Loo, J.N. Yao. Microstructures of electrochromic MoO₃ thin films colored by injection of different cations // *J. Phys. Chem. B*, 1998, 102(47), 9392-9396, DOI:10.1021/jp9825922-- <https://doi.org/10.1021/jp9825922>
3. Суровой Э.П., Борисова Н.В. Бугерко Л.Н. Суровая В.Э. РАМАЗАНОВА Г.О. // ФОТОСТИМУЛИРОВАННЫЕ ПРЕВРАЩЕНИЯ В НАНОРАЗМЕРНЫХ ПЛЕНКАХ МоО₃ // Журнал физической химии, 2013. Т.87, № 12. С. 2105–2109. DOI: 10.7868/S0044453713120273
4. Миннеханов А.А, Вахрина Е.В, Константинова Е.А, Кашкаров П.К. Особенности процессов накопления заряда в наногетероструктурах на основе оксидов титана и молибдена. // *Письма в ЖЭТФ*, Г. 2018 том 107, вып. 4, с. 270 – 275. http://www.mathnet.ru/php/archive.php?wshow=paper&jrnid=jetpl&paperid=5507&option_lang=rus#
5. S. Zhuiykov, *Nanostructured Semiconductor Oxides for the Next Generation of Electronics and Functional Devices: Properties and Applications*, Woodhead Publishing, Cambridge, UK, 2014, p. 484. DOI:10.1016/c2013-0-16486-0 Corpus ID: 134112610
6. Zhuiykov, S., Kats, E. Atomically thin two-dimensional materials for functional electrodes of electrochemical devices. *Ionics* 19, 825–865 (2013). doi.10.1007/s11581-012-0837-2
7. J. Z. Ou, S. Balendhran, M. R. Field, D. G. McCulloch, A. S. Zoofakar, R. A. Rani, S. Zhuiykov, A. P. O’Mullane and K. Kalantar-Zadeh, *Nanoscale*, 2012, 4, 5980–5988. doi.10.1039/C2NR31203D The anodized crystalline WO₃ nanoporous network with enhanced electrochromic properties
8. M. Osada and T. Sasaki, *Adv. Mater.*, 2012, 24, 210–223. doi.10.1002/adma.201103241 Two-Dimensional Dielectric Nanosheets: Novel Nanoelectronics From Nanocrystal Building Blocks
9. H. Zheng, Z. O. Jian, M. S. Strano, R. B. Kaner, A. Mitchel and K. Kalantar-zadeh, *Adv. Funct. Mater.*, 2011, 21, 2175–2196. doi.10.1002/adfm.201002477 Nanostructured Tungsten Oxide – Properties, Synthesis, and Applications
10. Гаврилюк А.И. Секушин Н.А. Электрохромизм и фотохромизм в



- оксидах вольфрама и молибдена// ЖТФ. – 1989. т. 15. Вып.2, с. 74-77
11. Колмакова Л.П. Ковтун О.Н. Довженко Н.Н. // Журн. Сиб. фед. ун-та. Техника и технологии 4 (2012 5) 472–483. Физико-химические основы взаимодействия присадочных компонентов с вольфрамовыми ангидридами
 12. Шиврин Г.Н. Прикладная квантовая химия. Рязань: НП «Голос губернии», 2009. 314 с.
 13. J. Martinez-Juárez and J. Díaz-Reyes "A method for deposition of tungsten trioxide (WO₃)", Proc. SPIE 7142, Sixth International Conference on Advanced Optical Materials and Devices (AOMD-6), 71420Q (2 December 2008); <https://doi.org/10.1117/12.815958>
 14. V. Hariharan et al. / «Synthesis of Tungsten Oxide (WO₃) Nanoparticles with EDTA by Microwave Irradiation Method» Int. J. Adv. Sci. Eng. Vol. 3 No.2 299-307 (2016) <https://www.researchgate.net/publication/311648951>
 15. N.M.G. Parreira Thin Solid Films 510 (2006) 191–196 doi:10.1016/j.tsf.2005.12.299
 16. Alov N.V. Surface oxidation of metals by oxygen ion bombardment Nucl. Instrum. // Methods Phys. Res. B. 2007. V. 256. Iss. 1. P. 337 DOI:10.1016/J.NIMB.2006.12.023 Corpus ID: 98554106
 17. Алов Н.В. Леонов М.П. Образование оксидов в поверхностных слоях молибдена и вольфрама в результате ионной имплантации кислорода // Физика и химия обработки материалов. 1986. Т. 6. № 6. С. 94